Interhyperhedral Diffusion in Josephson-Junction Arrays

Kwok Yeung Tsang and Ira B. Schwartz

U.S. Naval Research Laboratory, Special Project for Nonlinear Science, Code 4700.3, Washington, D.C. 20375-5000

(Received 15 May 1991)

We study the phase space for arrays of coupled Josephson-junction oscillators which have coexisting in-phase and antiphase attractors. Arrays with four or more oscillators have significantly different attracting sets from those with two or three: Continuous families of out-of-phase attractors can exist instead of isolated ones. A new mechanism in the presence of small amplitude noise is proposed to account for the observed transitions among different stable antiphase states, and the rarely observed transitions between an in-phase and an antiphase attractor.

PACS numbers: 05.40.+j, 05.45.+b, 74.40.+k, 74.50.+r

Nonlinear dynamical systems with many degrees of freedom have generated increasing attention recently. Coupled oscillators such as Josephson-junction arrays are of fundamental interest as examples of such systems. Josephson-junction arrays are superconducting electronic devices capable of generating oscillations in the GHz frequency range, and have the potential of applications as parametric amplifiers, high-frequency voltage generators, and voltage standards [1-3], as well as for generation of squeezed states in quantum electronics [4,5]. In these instances, one wishes that the junctions oscillate perfectly in phase [1,6-10]. Recent studies [11,12] show that, due to a dynamical symmetry, series arrays of point-contact Josephson junctions are unusually sensitive to random noise when shunted by a pure resistive load. In order to achieve the stability of the in-phase state, it is desirable to use an LC load.

When a series array of N identical point-contact Josephson junctions is subject to a constant bias current I_B and is shunted by an LC load, the governing dynamical equations are, in dimensionless form,

$$\dot{\varphi}_k+\sin\varphi_k+I=I_B,\quad k=1,\ldots,N, \tag{1}$$

$$L\dot{I}+Q/C=\sum_{j=1}^{N}\dot{\varphi}_j, \tag{2}$$

where φ_k is the phase difference in the electron wave function across the kth junction, $Q(t)=\int^t I(t')dt'$, and I, L, and C are respectively proportional to the current, inductance, and capacitance of the load. One important feature of these equations is the presence of "global coupling" wherein each oscillator is coupled with equal strength to all others. Notice the equations are invariant under permutations of the angular variables.

The in-phase (IP) state is defined by $\varphi_k(t)=\varphi_0(t)$ for all k. Parameters can be adjusted so that this state is an attractor [8]. There are also other types of out-of-phase (OP) attractors in which each junction oscillates with the same frequency, but $\varphi_j(t)\neq\varphi_k(t)$ for all $j\neq k$. An example of an OP attractor is the antiphase (AP) attractor, whose junctions oscillate with not only the same frequency, but also identical wave form. Moreover, in an array of N junctions, the existence of one stable AP state implies that there are $(N-1)!$ of them, due to the equivariant symmetry [9,13,14]. In a significant range of parameters, these two types of attractors coexist [8].

Recent numerical studies show that coupled nonlinear oscillators with equivariant symmetry can suffer a noise sensitivity that grows rapidly with the array size. It was suggested that the underlying cause is a phenomenon termed attractor crowding [9,13]. Its basic notion is that the existence of such a huge number of attractors can lead to a noise sensitivity due to competition between dynamical states. No matter how small the noise level, there is a limit to the size of the array beyond which noise corrupts the in-phase dynamical state. In order to understand such an effect, a complete picture of all the attractors in the phase space and their basins is needed [9].

In this Letter, we study systems of Josephson junctions described by Eqs. (1) and (2). As an effort to unfold the complete picture, we locate the attractors and identify their basins of attraction in the phase portraits. We show that there is a significant difference in the attracting sets between a system consisting of two or three junctions and one consisting of four or more. The observed structure for four or more junctions gives rise to a new form of motion under random noise, which explains why AP-AP transitions [8,13] are more readily seen than the rarely observed IP-AP transitions.

To study the phase portraits, we use array sizes $N=2,3,4$ and numerically integrate Eqs. (1) and (2) with the following parameters: $I_B=2.1$, $L=0.5N$, $C=0.5/N$. (The natural scaling [8] is so that the in-phase oscillations are independent of N.) The dynamics rapidly collapses onto a manifold whose projection onto the space $\{\varphi_1,\ldots,\varphi_N\}$ is an N torus. Physically, the initial I and Q relax rapidly to synchronize with the junction oscillations. Their wave forms then vary on a much slower scale.

Figure 1 shows the phase portrait for the two-junction array. We have used a set of transformed coordinates $x_0=(\varphi_1+\varphi_2)/2$, $x_1=(\varphi_2-\varphi_1)/2$. The rectangle shown is actually the torus $\{0\leq\varphi_1\leq 2\pi, 0\leq\varphi_2\leq 2\pi\}$ cut in a special way. The x_0 axis points to the direction in which all orbits proceed on the average. The top and bottom edges are two copies of the IP attractor. The solid curve is the AP attractor. The dashed curves are the repelling invariant orbits, which also mark the basin boundary of the two attractors.

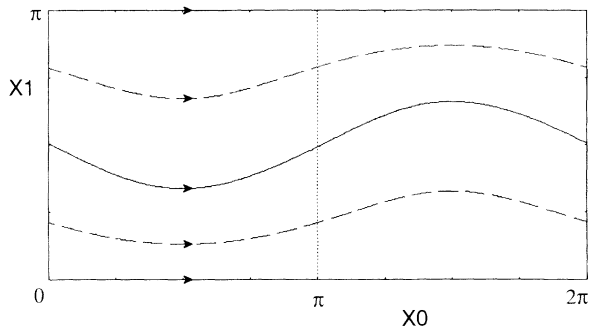

FIG. 1. Phase portrait for two-junction array. $x_0=(\varphi_1+\varphi_2)/2$ and $x_1=(\varphi_2-\varphi_1)/2$.

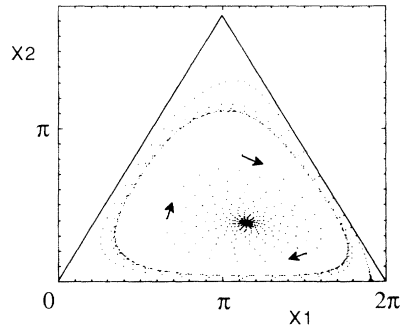

FIG. 2. Poincaré section of a canonical invariant region at $x_0=\pi(\mathrm{mod}2\pi)$ for the three-junction array. $x_0=(\varphi_1+\varphi_2+\varphi_3)/3$, $x_1=\varphi_3-(\varphi_1+\varphi_2)/2$, and $x_2=(\sqrt{3}/2)(\varphi_2-\varphi_1)$. The three vertices of the triangle have (clockwise beginning with the origin) $\varphi=(\pi,\pi,\pi)$, $(-\pi/3,5\pi/3,5\pi/3)$, and $(\pi/3,\pi/3,7\pi/3)$. The three sides correspond to (clockwise beginning with x_1 axis) the states $\varphi_1=\varphi_2$, $\varphi_2=\varphi_3$, and $\varphi_1+2\pi=\varphi_3$.

When more junctions are involved, the visualization of the consequently higher-dimensional phase portraits can be facilitated by considering the map defined by a Poincaré section $\bar{\varphi}=\sum\varphi_k/N=\pi(\mathrm{mod}2\pi)$. This map for the two-junction array will be on a line segment (which is dotted in Fig. 1). On the line segment lie an AP attractor, an IP attractor [two copies, corresponding to $\varphi=(\pi,\pi)$ and $(0,2\pi)$], and two repellers forming the basin boundaries of the former two.

When no noise is present, except perhaps for a very short transient, the dynamics with N junctions is observed to stay within one of the $(N-1)!$ regions of the N torus, each corresponding to an ordering of the phases. Because of the symmetry, we need only consider one of these regions to understand the whole picture. In particular, we consider the canonical invariant region (CIR) [15] corresponding to the condition $\varphi_1\le\varphi_2\le\cdots\le\varphi_N\le\varphi_1+2\pi$ at the Poincaré section $\bar{\varphi}=\pi$.

For the array with three junctions, we use the following orthogonal set of coordinates: $x_0=\bar{\varphi}$, $x_1=\varphi_3-(\varphi_1+\varphi_2)/2$, and $x_2=(\sqrt{3}/2)(\varphi_2-\varphi_1)$ [16,17]. Numerical results for the Poincaré section at $x_0=\pi$ of the CIR are shown in Fig. 2. The three vertices of the equilateral triangle are copies of the IP attractor. Near the centroid lies an AP attractor. A repelling invariant curve enclosing the AP attractor marks the basin boundary between the two attractors. An orbit with initial condition near and outside the curve is shown attracted to the IP state. The earlier stage of this orbit is not resolvable from the invariant curve (which is thus not plotted). Another orbit with initial condition well inside the curve is shown attracted to the AP state. The three edges represent the states with two identical φ_k's. Each edge has a saddle separating the orbits that go in opposite directions to the (same) IP attractor. (Recall that the orbits are on a torus.) In fact, the former orbit gets near the saddle before being attracted to the IP attractor along the edge. The Floquet multipliers at the fixed points are shown in Table I.

For the array with four junctions, we use these four orthogonal axes: $x_0=\bar{\varphi}$, $x_1=(-\varphi_1-\varphi_2+\varphi_3+\varphi_4)/4$, $x_2=(-\varphi_1+\varphi_2-\varphi_3+\varphi_4)/4$, and $x_3=(-\varphi_1+\varphi_2+\varphi_3-\varphi_4)/4$. As shown in Fig. 3, the Poincaré section of a CIR is a tetrahedron consisting of four identical isosceles triangles, each having sides of lengths $\frac{1}{2}\sqrt{3}\pi$, $\frac{1}{2}\sqrt{3}\pi$, and π. The four short edges of the tetrahedron represent the states where three of the four φ_k's are identical; the two long edges represent the states with two pairs of identical φ_k's. The vertices are IP attractors having $\varphi=(\pi,\pi,\pi,\pi)$, $(\pi/2,\pi/2,\pi/2,5\pi/2)$, $(0,0,2\pi,2\pi)$, and $(-\pi/2,3\pi/2,3\pi/2,3\pi/2)$. Numerical results show the existence of an attracting one-dimensional set of OP states, i.e., there is a filament linking two end points, one on each of the two long edges of the tetrahedron. Such filaments are sketched in Fig. 3. This is topologically different from the three-junction case. The OP curve represents a continuous (one-parameter) variation between two degenerate OP states, namely, $\varphi_1(t)=\varphi_2(t)=\varphi_3(t-T/2)=\varphi_4(t-T/2)$ and $\varphi_1(t)=\varphi_2(t-T/2)=\varphi_3(t-T/2)=\varphi_4(t-T)$. Here T is the period of the OP state. Notice that there exists a

TABLE I. Floquet multipliers λ at different fixed points for various array sizes N. The trivial multiplier $\lambda=1$ and a pair of complex conjugate $|\lambda|\cong0.05$ have been omitted in each cell. The multiplicity is shown in brackets.

N	In phase	Out of phase	Saddle,repeller
2	0.935	0.876	1.089
3	0.935 [2]	$0.9\pm0.4i$	<1
			>1
			On 4 short edges[b]
4	0.935 [3]	c.c. pair[a]	<1 [2]
		1	>1
			On N edges[d]
>4	0.935 [$(N-1)$]	c.c pair[c]	<1 [$(N-2)$]
		1 [$(N-3)$]	>1

[a]λ=complex conjugate pair ($0.9\pm0.4i$ at splay phase; $\rightarrow$ 0.876 [2] near degenerate OP).
[b]Two saddles on each long edge with $\lambda<1$; >1 [2].
[c]λ=complex conjugate pair ($0.9\pm0.4i$ at splay phase; $\rightarrow$ real pair near degenerate OP).
[d]Types of saddles on other edges more complicated [24].

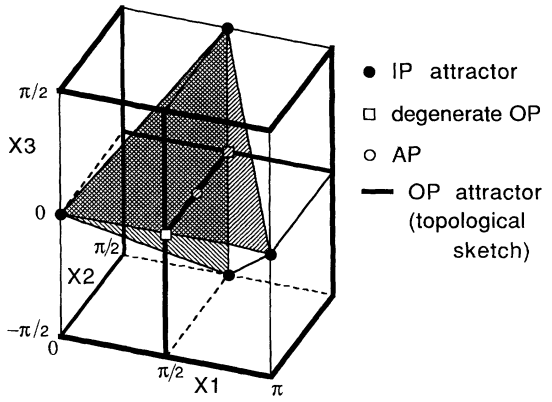

FIG. 3. Poincaré section at $x_0=\pi(\mathrm{mod}2\pi)$ for the four-junction array. $x_{0,1}=(\pm\varphi_1\pm\varphi_2+\varphi_3+\varphi_4)/4$, and $x_{2,3}=(-\varphi_1+\varphi_2\mp\varphi_3\pm\varphi_4)/4$. The three-torus is cut (and pasted) in a special way and shown as four cubes. It is equivalent to six copies of an invariant region such as the CIR shown, a tetrahedron. The OP filament joining the two degenerate OP states is inside the tetrahedron.

point on the attracting OP set which corresponds to the AP (bona fide splay phase) [10,18–21] state $\varphi_1(t)=\varphi_2(t-T/4)=\varphi_3(t-T/2)=\varphi_4(t-3T/4)$. The OP basin boundary is topologically equivalent to a cylinder enclosing the OP filament. Within the cylinder, there is a one-dimensional continuum (stack) of surfaces each having (near the center) a stable OP state into which trajectories spiral. Each surface also extends outside the cylinder, and merges with other such surfaces at the four short edges of the tetrahedron. On each of these edges, there is a saddle similar to those in the three-junction case. On each surface, the dynamics is similar to the triangle in the three-junction case.

Table I shows the Floquet multipliers at different fixed points. At each fixed point along the OP filament, the complex conjugate pair of Floquet multipliers is about 0.9 in magnitude. Orbits on the splay-phase surface appear to undergo weaker attraction, whereas orbits on the tetrahedron faces are subject to the strongest attraction to the degenerate OP states. Towards the edges, the pair of multipliers (at the filament) approaches a real number as the OP state approaches the degenerate OP state [22]. The Floquet multiplier $\lambda=1$ is a signature of linearly neutral stability along the OP filament. It is a reasonable conjecture that the stability between the surfaces should also be neutral.

For N larger than 4, the Poincaré section of the CIR is an $(N-1)$-dimensional hyperhedron with N vertices [17]. The behaviors at the IP and splay-phase fixed points are similar to those in the three-junction or four-junction cases. The Floquet multipliers are shown in Table I. The presence of $(N-3)$ OP Floquet multipliers $\lambda=1$ (up to single precision machine accuracy) suggests that there is a $(N-3)$-dimensional hypersurface of OP attractor [23]. Each point on the OP attractor has a two-dimensional surface as its own basin of attraction. On each surface there is a repelling limit cycle. Inside (respectively outside) the cycle, there is spiral motion toward the OP (respectively IP) attractor. Details of the phase portraits for a general N will be reported elsewhere [24].

Under the presence of noise, the difference between the three-junction and four-junction cases, though simple, is a significant one. Specifically, we model the noise by adding a random term $\sqrt{\kappa}\xi_k(t)$ to Eq. (1), representing the noise current due to the individual junction resistances. The $\xi_k(t)$ are independent δ-correlated random functions with zero mean and unit variance; κ is proportional to the power of each noise source. Figure 4 shows the diffusionlike motion along the filament from the AP towards the degenerate OP state. We are now ready to explain why it has been numerically observed under random noise that the dynamics easily hops among different stable AP states, but less so from IP to AP states [13]. In particular, with at least four junctions, the latter requires that the noise overcomes the attraction of the IP attractor (and the repulsion of the basin boundary); while the former can be achieved merely by motion along the neutrally stable continuum. An orbit initially at, say a splay-phase state, can easily drift along the neutrally stable direction to a degenerate OP state on the edge of the hyperhedron, where several hyperhedrons meet. It can then easily drift further under diffusion into another hyperhedron along another neutrally stable direction. We call this effect the *interhyperhedral diffusion.* In fact, the diffusion is due to noise which causes the system to random walk all over the web of OP filaments. What happens physically, in the four-junction case, for instance, is that four OP filaments meet at each degenerate OP fixed point (see Fig. 3), corresponding to two possible symmetry breakings for each pair of degenerate junctions. If the noise kicks the system into a state along a filament other than the one the system came from, there will be a switch in the ordering of the oscillators. This phenomenon, while not deterministic because noise is involved, is similar to Arnold diffusion [25] in the sense that it occurs only in sufficiently high degrees of freedom. Numerically simulations verify that an AP-AP transition is relatively easily observed as opposed to an IP-AP one. We predict that the effect can be seen also in experiments

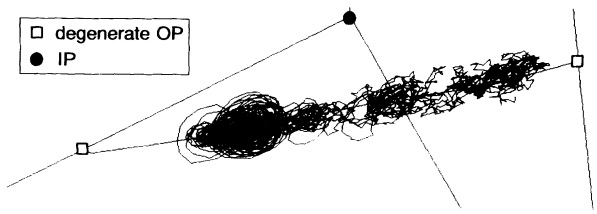

FIG. 4. Diffusion under random noise along the OP attractor in the Poincaré section at $x_0=\pi(\mathrm{mod}2\pi)$ for the four-junction array. Succession points are connected to facilitate visualization.

possessing similar symmetry invariants to Eqs. (1) and (2), such as globally coupled laser systems [26,27]. More general, but abstract, systems possessing generic equivariant vector fields with $N=4$, also have invariant OP filaments in the absence of noise [21]. We predict, therefore, that interhyperhedral diffusion will occur in systems where oscillators with $N \geq 4$ possess an equivariant symmetry. Other imperfect systems lacking symmetry in the coupling also are observed to exhibit diffusion in the presence of noise [24].

Visualizing the phase portraits is very important in understanding the dynamics of coupled oscillators. As we go from two junctions to three, four, and N, a more complete picture is gradually unveiled. By focusing on one CIR, which contains only $[(N-1)!]^{-1}$ of the OP attracting set [28], we can now avoid the complexity due to the multiplicity of OP states.

We have now also laid down the ground work to study not only the effect of noise but also the effect of array size under constant noise strength. This enhances the potential of understanding the cause of the attractor crowding effect [9,13].

We would like to thank Horace Mitchell, Shou-Li Peng, Steve Strogatz, Jim Swift, and Kurt Wiesenfeld for stimulating discussions. This work was supported by the Office of Naval Research, the Office of Naval Technology, and the American Society for Engineering Education.

[1] A. K. Jain, K. K. Likharev, J. E. Lukens, and J. E. Sauvageau, Phys. Rep. **109**, 310 (1984), and references therein.

[2] R. L. Kautz, C. A. Hamilton, and F. L. Lloyd, IEEE Trans. Mag. **23**, 883 (1987).

[3] C. A. Hamilton, R. L. Kautz, F. L. Lloyd, R. L. Steiner, and B. F. Field, IEEE Trans. Instrum. Meas. **36**, 258 (1987).

[4] B. Yurke, P. G. Kaminsky, R. E. Miller, E. A. Whittaker, A. D. Smith, and R. W. Simon, Phys. Rev. Lett. **60**, 764 (1988).

[5] B. Yurke (private communication).

[6] P. Hadley and M. R. Beasley, Appl. Phys. Lett. **50**, 621 (1987).

[7] P. Hadley, M. R. Beasley, and K. Wiesenfeld, Phys. Rev. B **38**, 8712 (1988).

[8] P. Hadley, Ph.D. dissertation, Stanford University, 1989 (unpublished).

[9] K. Y. Tsang and K. Wiesenfeld, Appl. Phys. Lett. **56**, 495 (1990).

[10] K. Y. Tsang, R. E. Mirollo, S. H. Strogatz, and K. Wiesenfeld, Physica (Amsterdam) **48D**, 102 (1991).

[11] K. Y. Tsang, S. H. Strogatz, and K. Wiesenfeld, Phys. Rev. Lett. **66**, 1094 (1991).

[12] K. Y. Tsang and K. Wiesenfeld, J. Appl. Phys. **70**, 1075 (1991).

[13] K. Wiesenfeld and P. Hadley, Phys. Rev. Lett. **62**, 1335 (1989).

[14] D. G. Aronson, M. Golubitsky, and M. Krupa, Nonlinearity **4**, 861 (1991).

[15] P. Ashwin and J. W. Swift, J. Nonlin. Sci. **2**, 69 (1992).

[16] P. Ashwin, G. P. King, and J. W. Swift, Nonlinearity **3**, 585 (1990).

[17] The recipe of the coordinate transformation for a general N is addressed in a separate article: K. Y. Tsang (unpublished).

[18] R. E. Mirollo, "Splay-Phase Orbits for Equivariant Flows on Tori" (unpublished).

[19] D. G. Aronson, M. Golubitsky, and J. Mallet-Paret, Nonlinearity **4**, 903 (1991).

[20] J. W. Swift, S. H. Strogatz, and K. Wiesenfeld, Physica (Amsterdam) D (to be published).

[21] M. Field and J. W. Swift, Nonlinearity **4**, 1001 (1991).

[22] Trajectories on an edge remain on it. (So do those on a face.) The presence of orbits attracted to the degenerate OP state along the edge from opposite directions requires that the Floquet multipliers be real.

[23] Quasi-Newton techniques have been applied to ensure that points on an OP attractor are fixed points rather than part of a long transient.

[24] K. Y. Tsang and I. B. Schwartz (to be published).

[25] V. I. Arnold, Sov. Math. Dokl. **5**, 581 (1964).

[26] K. Wiesenfeld, C. Bracikowski, G. James, and R. Roy, Phys. Rev. Lett. **65**, 1749 (1990).

[27] K. Otsuka, Phys. Rev. Lett. **67**, 1090 (1991).

[28] In the case of N junctions, a total of $(N-1)!$ copies of the CIR are needed to form the N torus. As we can see when $N=3$, the CIR (as well as every IR) contains one AP orbit and its entire attraction basin. Nevertheless, despite possessing three copies of the IP attractor in the three-junction case (in Fig. 2), the CIR only includes $\frac{1}{6}$ (60° out of 360°) of the basin of attraction at each vertex. Similarly, for a general N, the CIR contains one splay-phase orbit and its entire attraction basin. However, even though the CIR contains N copies of the IP attractor, only a fraction, i.e., $[(N-1)!]^{-1}$, of the attraction basin is included. In other words, we see exactly $[(N-1)!]^{-1}$ of the torus in one CIR.